CADHERIN mediated AMIS localisation

Xuan Liang[1], Antonia Weberling[1], Chun Yuan Hii[1], Magdalena Zernicka-Goetz[1,2], Clare Buckley[1#]

[#] Corresponding author

[1] Department of Physiology, Development and Neuroscience
University of Cambridge
Downing Street
Cambridge
CB2 3BY

[2] Division of Biology and Biological Engineering
Caltech
Pasadena

Abstract

Individual cells within *de novo* polarising tubes and cavities must integrate their forming apical domains into a centralised apical membrane initiation site (AMIS). This is necessary to enable organised lumen formation within multi-cellular tissue. Despite the well documented importance of cell division in localising the AMIS, we have found a division-independent mechanism of AMIS localisation that relies instead on CADHERIN-mediated cell-cell adhesion. Our study of *de novo* polarising mESCs suggest that cell-cell adhesion directs the localisation of apical proteins such as PAR-6 to a centralised AMIS. Unexpectedly, we also found that mESC cell clusters lacking functional E-CADHERIN were still able to form a lumen-like cavity in the absence of AMIS localisation and did so at a later stage of development via a 'closure' mechanism, instead of via hollowing. This work suggests that there are two, interrelated mechanisms of apical polarity localisation: cell adhesion and cell division. Alignment of these mechanisms allows for redundancy in the system and ensures the localisation of a coherent epithelial structure within a growing organ.

Introduction

Most organs in the body arise from tubes or cavities made from polarised epithelial cells. These cells have a strict apico-basal orientation; they align their apical ends along a centrally located lumen. Some tubes, such as the anterior neural tube in amniotes, arise via folding and closure of an already polarised epithelial tissue, through mechanisms such as actomyosin-mediated apical constriction (Nikolopoulou et al., 2017). However, many tubes and cavities, such as the posterior neural tube, mammary acini, kidney tubules and mammalian epiblast arise via apical-basal polarisation within the centre of an initially solid tissue. The mechanisms by which such '*de novo'* polarisation is coordinated within dynamically growing tissue has been the focus of a significant body of research from several different models and have relevance both for understanding polarity-associated diseases and for directing organ bioengineering approaches.

Although the exact mechanisms are still under debate and may differ in different epithelia, LAMININ, INTEGRIN β1 and RAC1 signalling from the extra cellular matrix (ECM) is now well established to be necessary for directing the overall apico-basal axis of polarisation of internally polarising tubes (Akhtar and

Streuli, 2013; Bedzhov and Zernicka-Goetz, 2014; Bryant et al., 2014; Buckley et al., 2013; Molè et al., 2021; Yu et al., 2005). What is less clear is how the precise localisation of the apical membrane initiation site (AMIS) is directed at the single cell level and how this is coordinated between neighbouring cells. The AMIS is a transient structure, marked by the scaffolding protein PARTITIONING DEFECTIVE-3 (PAR-3) and tight junctional components such as ZONULA OCCLUDENS-1 (ZO-1), that defines where apically targeted proteins will fuse with the membrane, therefore determining where the lumen will arise (Blasky et al., 2015; Bryant et al., 2010). It is important that the subcellular localisation of the AMIS is coordinated between cells during morphogenesis to enable organised lumen formation.

The current literature suggests that cell division plays an important role in AMIS localisation. In particular, the post-mitotic midbody has been shown to anchor apically directed proteins (Li et al., 2014; Luján et al., 2016; Rathbun et al., 2020; Schlüter et al., 2009; Wang et al., 2014). However, studies within the zebrafish neural rod showed that, whilst misorientation of cell division results in disruption of the apical plane at a tissue level, these phenotypes can be rescued by inhibiting cell division (Ciruna et al., 2006; Quesada-Hernandez et al., 2010; Tawk et al., 2007; Zigman et al., 2011). We also previously demonstrated that individual zebrafish neuroepithelial cells were able to recognise the future midline of the neural primordium and organise their intracellular structure around this location in advance and independently of cell division. This resulted in the initiation of an apical surface at whichever point the cells intersect the middle of the developing tissue, even if this is part way along a cell length (Buckley et al., 2013). This suggests that, while cell division is undoubtably a dominant mechanism in driving AMIS localisation, there must be an overlying symmetry-breaking event during *de novo* polarisation. The earliest indication of midline positioning in the zebrafish neural rod was the central accumulation of the junctional scaffolding protein Pard3 and the adhesion protein N-Cadherin (Buckley et al., 2013; Symonds et al., 2020). This led us to hypothesise that cell-cell adhesions could direct the site for AMIS localisation during *de novo* polarisation. In line with this hypothesis, β-catenin mediated maturation of N-cadherin was found to be necessary for the recruitment of the PAR apical complex protein atypical PROTEIN KINASE C (aPKC) in the chick neural tube (Herrera et al., 2021). Opposing localisations of ECM and CADHERIN proteins were also found to be sufficient to specify the apical-basal axis of hepatocytes in culture (Zhang et al., 2020).

To test the role of cell-cell adhesions in AMIS localisation, we turned to mouse embryo stem cell (mESC) culture in Matrigel, which has been used as an *in vitro* model for the *de novo* polarisation of the mouse epiblast (Bedzhov and Zernicka-Goetz, 2014; Kim et al., 2021; Molè et al., 2021; Shahbazi et al., 2017). This allowed us to study the initiation of apico-basal polarity of embryonic cells alongside the first cell-cell contacts between isolated cells and small cell clusters. It also allowed us to determine within a mammalian model whether division-independent polarisation is a conserved feature of *de novo* polarising structures. Unlike vertebrate epithelial cell culture models such as Madin-Darby canine kidney (MDCK) cells, which initiate lumenogenesis as early as the 2-cell stage when cultured in Matrigel (Blasky et al., 2015; Bryant et al., 2010), mESC cells in Matrigel only form lumens at the multicellular stage after 48-72 hours in culture, coinciding with an exit in pluripotency (Bedzhov and Zernicka-Goetz, 2014; Shahbazi et al., 2017). This results in a relatively clear separation of the stages of *de novo* polarisation (figure 1A). Previous literature suggests that the AMIS is formed at the 2-cell stage, around 24-36 hours after culture in Matrigel, as denoted by membrane-localised PAR-3 and ZO-1 and sub-apical localisation of apical proteins such as PODOCALYXIN (PODYXL) (Shahbazi

et al., 2017). The pre-apical patch (PAP) stage is formed after 36-48 hours in culture, as denoted by the fusion of apical proteins such as PODXYL, PAR-6 and aPKC to the apical membrane and the displacement of junctional proteins PAR-3, ZO-1 and E-CADHERIN to the apico-lateral junctions (Kim et al., 2021; Shahbazi et al., 2017), following which lumenogenesis is initiated after 48-72 hours in culture.

To determine the role of cell division and of cell adhesion in mESC AMIS localisation, we analysed mESC cells cultured in Matrigel at the 24-hour AMIS stage with and without cell division in wild type and E-CADHERIN knock out cell lines. We then further analysed polarisation and lumenogenesis in the absence of E-CADHERIN. Our results suggest that there is a division-independent mechanism of AMIS localisation that relies instead on E-CADHERIN mediated cell-cell adhesions.

Results

Cell division is dispensable for AMIS localisation

First, we tested whether cell-division was necessary for AMIS localisation in mESC rosettes. We cultured naïve, unpolarized mESCs in 2D on gelatin with 2i/LIF and then treated them with mitomycin C to block cell division. We then isolated single cells and seeded them into Matrigel without 2i/LIF, in N2B27 differentiation medium (Figure 1B). Cell divisions were efficiently blocked during the first 24 hours post seeding, during which time individual cells contacted each other and formed cell clusters in the absence of cell division (Supplementary Movie 1, Figure S1 A,B).

To assess AMIS localisation, we carried out immunohistochemistry (IHC) for PAR-3 and ZO-1 at 24hrs post seeding. As previously published (Shahbazi et al., 2017), in addition to several puncta at the cell peripheries, both PAR-3 and ZO-1 localised to the membrane at the centre of cell-cell contacts, marking the AMIS in the majority of cell clusters (Figure 1Ci,Gi and S1E,F). Interestingly, division-blocked cells also localized PAR-3 and ZO-1 to the central membrane (Figure 1Cii,Gii, and S1E,F, quantified in 1D,I). In both control and division-blocked cells, there was a small proportion that had not yet localised the AMIS at the 24-hour stage (Figure 1D,I & S1D). E-CADHERIN was upregulated along the whole length of the cell-cell interfaces in both dividing and non-dividing cell clusters, with a higher level of E-CADHERIN at the cell-cell interface relative to the cell-matrix interface (Figure 1C and S1C,E). To quantify the subcellular localization of PAR-3, we carried out intensity profiles across the cell-cell interface of doublets (Figure 1F). This confirmed that PAR-3 localised to a small central area at the cell-cell interface in both control and division-blocked cells (Figure 1E and 3C). Golgi apparatus and centrosomes were also localised to the centre of cell-cell contacts both in dividing and non-dividing conditions (Figure 1G-J & S1F), confirming that mESCs were polarised in the absence of cell-division.

Together, these results demonstrate that cell division is dispensable for *de novo* AMIS localisation in polarizing mESCs.

Cell-cell contact directs PAR-6 localisation

To understand the dynamics of apical protein polarisation in the absence of cell division, we generated a mESC stable cell line expressing mCherry-PAR-6B and imaged cells live. In line with previous characterisation of

PAR-6 by IHC (Kim et al., 2021; Shahbazi et al., 2017), in control dividing cells, mCherry-PAR-6B localized to the apical membrane by the PAP stage at 48 hours and to the luminal apical membrane from 72h (Figure 2A). In addition, the transgene allowed us to better visualize PAR-6B puncta at earlier 24h AMIS stages of development, before they had associated with the apical membrane. At this stage, PAR-6B was localized sub-apically, polarized to towards the central region of cell-cell contact (Figure 2A). A similar polarised distribution of PAR-6B was observed in both control and division-blocked cells (Figure 2B,C), demonstrating that cell division is dispensable for apical protein polarisation.

We next assessed the dynamics of PAR-6B polarisation. In both control and division-blocked cells, non-cortical mCherry-PAR-6B puncta were visible at the single cell stage. In control cells, these puncta then relocalised to the abscission plane, following cell division (Figure 2D, supplementary movie 2). In division-blocked cells, PAR-6B puncta dynamically relocalised to newly forming cell-cell contacts, eventually forming cell-cell clusters with centrally localised PAR-6B (Figure 2D, supplementary movie 2).

These results suggest that cell-cell contact directs PAR-6B localisation at the central AMIS, independent of cell division.

E-CADHERIN is necessary for AMIS localisation

The above results suggest that there is an overlying, division-independent mechanism of AMIS localisation that relies instead on cell-cell adhesions. Since E-CADHERIN is the predominant adhesion molecule in non-neural epithelia, we hypothesised that it might be important in AMIS localisation. To test this, we employed an *E-Cadherin* knock-out (*Cdh1* KO) mESC line (Larue et al., 1996). Whilst E-CADHERIN expression was lost in *Cdh1* KO cells, they maintained P-CADHERIN expression (Figure S2A) and were still able to form cell clusters when cultured in Matrigel (Figure S2B).

To assess AMIS localisation, we again carried out IHC for PAR-3 and ZO-1 at 24hrs post seeding. As seen earlier (Figure 1), both PAR-3 and ZO-1 localised to the central region of cell-cell contact within control cell doublets and clusters with and without division. However, PAR-3 and ZO-1 localisation was strongly inhibited in the absence of E-CADHERIN (Figure 3). To investigate AMIS localisation at a single cell level, we co-cultured division-blocked wild type and *Cdh1* KO cells and analysed division-blocked chimeric mESC doublets, comprising one control and one *Cdh1* KO cell. Whilst homogenous control doublets localised PAR-3 to the central region of the cell-cell interface, heterogeneous chimeric doublets did not localise PAR-3 centrally (Figure 3D,E). Golgi and centrosome localisation towards the cell-cell interface suggested that the overall axis of polarity was maintained, even in the absence of both cell division and E-CADHERIN (Figure 3F-H & S2C).

It has previously been demonstrated that a reduction in E-CADHERIN can slow pluripotency exit (Soncin et al., 2009). However, pluripotency exit was previously shown not to alter AMIS formation (Shahbazi et al., 2017). In support of these results, we also found that cells maintained in the pluripotent state when cultured in the Feeder cell medium provided with 2i/LIF still localised the AMIS, with and without cell division. However, in line with our results showing lack of AMIS localisation in *Cdh1* KO cells cultured in the absence of 2i/LIF (Figure 3), cells cultured in the presence of 2i/LIF also could not localise an AMIS in the absence of E-CADHERIN (Figure S2E-F). We wanted to check whether the stage of pluripotency exit differed between WT and *Cdh1*

KO cells in our experiments since this might indicate a different speed of maturation. We therefore carried out IHC for Orthodenticle Homeobox 2 (OTX2) protein, which is necessary for pluripotency exit. Although, as expected, the overall level of nuclear OTX2 increased over the course of development, we found no significant difference in post-mitotic levels of OTX2 between WT and *Cdh1* KO cells (Figure S2G). This result suggests that there was no difference in the stage of pluripotency exit in the cell clusters that we analysed during this study and this is therefore unlikely to play a role in the lack of AMIS localisation seen in *Cdh1* KO cells.

These results demonstrate that E-CADHERIN adhesions between cells are necessary for AMIS localisation but not for the overall axis of polarity. The also demonstrate that ECM in the absence of E-CADHERIN is insufficient for AMIS localisation.

E-CADHERIN is sufficient for AMIS localisation, independent of ECM signalling and cell division

As discussed, ECM-mediated signalling plays an important role in orienting the axis of polarisation within *de novo* polarising systems. Recently, the apico-basal axis of cultured mature hepatocytes was established by a combination of ECM signalling and immobilised E-CADHERIN (Zhang et al., 2020). However, PAR-3 has also recently been shown to polarise in mESCs lacking functional INTEGRIN-β1 or cultured in agarose in the absence of ECM proteins (Molè et al., 2021). Our current study shows that the AMIS can localise in the absence of cell division but not in the absence of E-CADHERIN. We therefore wanted to explore the relative roles of ECM, cell division and E-CADHERIN in AMIS localisation.

To test this, we first eliminated the influence of ECM by culturing division-blocked mESCs in 0.5% Agarose and carried out IHC for PAR-3 after 30 hours in culture. These cells were still able to polarise PAR-3, even in the absence of both cell division and ECM proteins (Figure 4A,B). However, in line with our earlier results (Figure 3), PAR-3 localisation was strongly inhibited in *Cdh1* KO cells (Figure 4A,B). These results suggest that AMIS localisation occurs independently of both ECM signalling and of cell division, relying instead on E-CADHERIN.

To test the sufficiency of E-CADHERIN in directing AMIS localisation, we cultured individual division-blocked mESCs onto either E-CADHERIN-FC recombinant protein or FIBRONECTIN pre-coated glass, then topped the cells with N2B27 medium, with or without 30% Matrigel and carried out IHC for PAR-3 after 24 hours in culture. Like results from hepatocytes (Zhang et al., 2020), cells plated on E-CADHERIN and topped with Matrigel localised PAR-3 to the centre of the cell-CADHERIN interface (Figure 4Ci,D,E). However, this central PAR-3 localisation was significantly reduced when cells were plated on FIBRONECTIN (Figure 4Cii,D,E). Interestingly, cells cultured on E-CADHERIN but in the absence of Matrigel still localised PAR-3 to the centre of the cell-CADHERIN interface (Figure 4 Ciii,D,E).

These results demonstrate that E-CADHERIN is both necessary and sufficient for AMIS localisation, while ECM is not necessary or sufficient for AMIS localisation.

E-CADHERIN is necessary for hollowing lumenogenesis

We next wanted to test the importance of E-CADHERIN-mediated AMIS localisation in lumenogenesis. We therefore cultured WT and *Cdh1* KO mESCs and fixed them at the AMIS 24-hour stage, PAP 48-hour stage

and lumen 72 and 96-hour stage. We then carried out IHC for PAR-3 and ZO-1 to label AMIS/apicolateral junctions and PODXYL to label apical proteins. Whilst most WT cell clusters had a centralised apical domain or small lumen after 48 hours in culture, very few *Cdh1* KO cell clusters had made a centralised apical domain by the 48-hour PAP stage (Figure 5A-D). In line with our earlier findings at the 24-hour AMIS stage (Figure 3), this provides further evidence that E-CADHERIN is necessary for centralised AMIS localisation. However, we noticed that a small percentage of *Cdh1* KO cell clusters at 48 hours had formed an open 'cup-shape', with apically localised PODXYL and apico-laterally localised junctional PAR-3 and ZO-1 (e.g. figure 5Aiii). We termed these 'open cavities' (Figure 5C). Surprisingly, by the 72-hour lumen stage, approximately 75% of *Cdh1* KO cell clusters had formed polarised cavities, approximately 50% of which were open cavities and 50% were closed (Figure 5A-E). Over the course of 48-96 hours in culture, the overall percentage of polarised cavities increased (Figure 5D) as did the proportion of these structures that were 'closed' (Figure 5E). This suggested that these cavities might form via gradual 'closure' of the tissue, rather than via hollowing. Both 'open' and 'closed' cavities were surrounded by polarised Golgi apparatus, demonstrating that the overall apico-basal axis of cells was in-tact. (Fig. S3).

To further assess the morphogenetic mechanism by which cavities form in *Cdh1* KO cells, we generated WT and *Cdh1* KO mESC lines labelled with LifeAct-mRuby. We visualised the process of lumenogenesis within mESCs cultured in Matrigel via live imaging. Whilst the WT cell cluster expanded the already central lumen, the open cup-shaped cavity within *Cdh1* KO cell clusters gradually closed, eventually generating a centralised lumen-like structure without hollowing at a later stage of development (Figure 5F and supplementary movie 4).

These results confirm that, in the absence of E-CADHERIN mediated AMIS localisation, cell clusters do not hollow but instead generate lumen-like cavities via a closure mechanism (Figure 5G). Our results also demonstrate that E-CADHERIN and centralised AMIS localisation are not required for apical membrane formation. In the absence of E-CADHERIN, an apical surface is still formed but this occurs later in development so appears less efficient.

Discussion

Epithelial cells can polarise *de novo* in the absence of cell division.

Both AMIS associated proteins PAR-3/ZO-1 and apical polarity protein PAR-6b localised similarly in WT and division-blocked mESCs (Figures 1 and 2). This finding supports our previously published zebrafish neuroepithelial cell *in vivo* analysis, which demonstrated the division-independent localisation of Pard3 and ZO-1 at the neural rod primordial midline (Buckley et al., 2013). Together this demonstrates that although division is an important contributor to AMIS formation, a division-independent mechanism of *de novo* polarisation and AMIS localisation can occur in both *in vivo* and *in vitro* conditions. Whilst disorganised lumen formation can also occur in the absence of division in the zebrafish neural rod (Buckley et al., 2013), this was not possible to test within the mESC culture model since Mitomycin treated cell clusters did not survive beyond 30 hours in culture.

E-CADHERIN is necessary and sufficient for AMIS localisation

AMIS localisation in *Cdh1* KO cell clusters is strongly inhibited (Figure 3) and individual mESC cells can direct their AMIS to the central region of the cell-CADHERIN interface independently from ECM-signalling (Figure 4). Together this demonstrates that E-CADHERIN is both necessary and sufficient for AMIS localisation and that ECM is insufficient to direct AMIS localisation in the absence of CADHERIN. Our results therefore suggest that CADHERIN-mediated cell-cell adhesion may provide the symmetry-breaking step required for AMIS localisation during *de novo* polarisation. This in turn directs apical proteins such as PAR-6B to a centralised region of cell-cell contact (Figure 2), determining where the lumen will hollow.

Whilst we demonstrate that AMIS localisation can occur independently from cell division, the importance of abscission and midbody formation in apical protein targeting has been robustly demonstrated and the molecules involved are now starting to emerge (Klinkert et al., 2016; Li et al., 2014; Luján et al., 2016; Mangan et al., 2016; Rathbun et al., 2020; Schlüter et al., 2009; Wang et al., 2021, 2014). Rather than acting as the initial symmetry breaking step in AMIS localisation, we suggest that tethering of apically directed proteins to the midbody might instead act to transiently align cell division, cell adhesion and the apical domain, therefore enabling an organised structure to be generated in the presence of dynamic cell movement and tissue growth. The transient localisation of scaffolding and tight junction-associated proteins such as PAR-3 and ZO-1 at the AMIS might aid in this alignment. For example, CINGULIN is a tight junctional protein that has been shown to bind both to the midbody and to FIP5, which is important for the apical targeting of vesicles containing apical proteins (Mangan et al., 2016). During zebrafish neural rod development, cell adhesion and cell division align to allow an organised structure to arise from dynamically reorganising cells (Symonds and Buckley 2020) and loss of N-cadherin results in mis-oriented cell divisions and a disrupted apical domain (Zigman et al., 2011). Once apical proteins fuse with the apical membrane, proteins associated with junctions such as CADHERIN, PAR-3 and ZO-1 are then cleared from the apical surface and instead form the apicolateral junctions, as demonstrated in several different epithelial systems (Kim et al., 2021; Morais-de-Sa et al., 2010; Symonds et al., 2020).

Whilst we have demonstrated that E-CADHERIN directs AMIS localisation, we do not yet have an explanation for why AMIS proteins localise at the central-most point of cell-cell contact in the absence of divisions, despite E-CADHERIN localisation all along the cell-cell interface. PAR-3 and PAR-6 have been found to be directly recruited to CADHERIN proteins within endothelial cells (Iden et al., 2006). Recently, opposing actin flows in migrating cells as they first encounter each other were found to be responsible for regulating the first AJ deposition via tension-mediated unfolding of a-catenin and further clustering of surface E-CADHERIN molecules (Noordstra et al., 2021). Together, this could provide an explanation for how the first contacts between cells could act as an apical ‘seed’, therefore defining the position of the AMIS within multicellular tissues. This could therefore explain why we have previously seen an upregulation of N-Cadherin at the zebrafish neural rod midline, where cells growing from either side of the organ primordium meet (Symonds et al., 2020). However, it is still unclear how this might regulate the subcellular localisation of the AMIS to the centre of cell-cell contacts. It is possible that there is a differentially higher pattern of tension at this most central point of contact between two adhering cells. In line with this hypothesis, previous publications have demonstrated an upregulation of phosphorylated MYOSIN-II (pMLC) at the AMIS (Molè et al., 2021).

In the absence of an AMIS, lumens form via ‘closure’ rather than hollowing

The centralised localisation of an AMIS appears necessary to enable lumen hollowing within multi-cellular clusters. *Cdh1* KO cells lack AMIS localisation at the 24-hour AMIS stage (Figure 3). However, they still retain their apico-basal polarity axis (as denoted by Golgi apparatus and centrosome localisation, Figure 3F-H & S2C) and form apico-lateral junctions at luminal stages of development (from approximately 72 hours in culture, Figure 5). Therefore, *Cdh1* KO cells do appear to still make an apical membrane but do so more slowly than in WT cells and without going through a centralised AMIS stage. This suggests that the role of E-CADHERIN in *de novo* polarisation is specifically to localise the AMIS, which enables the integration of individual cell apical domains to a centralised region preceding lumen hollowing. The lack of a centralised AMIS in CADHERIN deficient cells could also explain the multiple-lumen (but otherwise polarised) phenotypes previously seen in E-CADHERIN deficient MDCK cells cultured on collagen (Jia et al., 2011).

A surprising observation was the ability of *Cdh1* KO mESC clusters, in the absence of AMIS localisation, to instead form 'lumen-like' structures via a 'closure' process. We do not currently know the mechanism by which such 'closure' occurs. However, the presence of F-ACTIN and p-MLC rich cable-like structures in 'cup'-shaped open cavities is potentially suggestive of a contractile process (Figure S3). Understanding the relative roles of mechanics in localisation of the AMIS and in 'opening' vs. 'closing' tubes is an important future research goal, as is the potential role of cell geometry in mediating such differences. Additionally, collective cell migration could play a role in this 'closure' mechanism. Collective inwards migration of cells caused lumen formation via a folding mechanism when MDCK monolayers were overlaid with a soft collagen gel (Ishida et al., 2014). A similar collective process could be occurring in the *Cdh1* KO cell clusters from our study, which were cultured in a soft (20%) Matrigel and formed loosely connected cell clusters, which then 'closed' to make a centralised lumen.

In summary, our work suggests that CADHERIN-mediated cell-cell adhesion provides a symmetry breaking event, necessary for localising the AMIS during *de novo* polarisation of epithelial tubes and cavities. Our work also suggests that ECM is insufficient to direct AMIS localisation in the absence of CADHERIN. In parallel with the well described role of the midbody in tethering apical proteins, this suggests that there are two, interrelated mechanisms of AMIS localisation: cell adhesion and cell division. The alignment of these cellular processes allows for redundancy in the system and provides an explanation for how an organised epithelial structure can arise within the centre of a proliferating organ primordium.

Material and Methods

Cells

The wild-type mESC (ES-E14) was purchased from Cambridge Stem Cell Institute. The Cdh1 KO mESCs were gifted from Lionel Larue lab at Institute Curie. mESC carriers were maintained in Feeder Cell Medium in Corning cell culture dishes precoated with 0.1% Gelatin (ES-006-B, Sigma-Aldrich), at 37 ℃ suppled with 5% CO_2 at one atmospheric pressure. The culture medium was renewed every three days. The cells were trypsinized when reaching confluency to be passaged or subjected to experiments.

Mouse PAR-6B CDS cDNA were assembly with mCherry by Gibson assembly, LifeAct-Ruby cDNA were sub-cloned from an existing plasmid. The cDNAs were cloned into pDONR221 plasmid and introduced into the PB-Hyg-Dest plasmid using Gateway technology (Thermo Fisher Scientific). The PB-Hyg-Dest-mCherry-PAR-6B or the PB-Hyg-Dest-LifeAct-Ruby plasmid were co-transfected with the piggyBac plasmid using Lipofectamine 3000 to generate Hygromycin B resistant stable cell lines. The mCherry-PAR-6B or LifeAct-Ruby expressing mESC stable cell line was created via 10 μg/mL Hygromycin B selection and single cell colonies expansion.

Cell cultures and treatment

For 3D culture of wild-type and E-cadherin knock-out mESCs, 20μL of Matrigel (356231, Corning, Lot 354230, 354234, 356231) was spread evenly to the bottom of each well in a μ-slide 8 well dish (80821, Ibidi). The dish was left on ice for 10 minutes to flatten, then was left at 37 ℃ for 10 minutes to solidify the Matrigel surface. mESCs were trypsinized, pipetted thoroughly and passed through a cell strainer (431750, Corning) to isolate cells into single cells. Singled mESCs were suspended in the N2B27 medium and seeded onto the solidified Matrigel. The seeded density was control, 14 cells/mm^2; Mitomycin C treated, 227 cells/mm^2. The cells were left at 37℃ for 15min when over 95% of the cells attached to the Matrigel, then the culture medium was renewed to 10% Matrigel/N2B27 medium with or without 2i/Lif.

For control and Cdh1 KO mESC chimeric clump cultures, wild-type and Cdh1 KO mESCs were mixed at 1:4 ratio and co-cultured at 2D in the Feeder Cell Medium. They were then treated with Mitomycin C for 2 hours, then trypsinized and seeded for 3D Matrigel culture at 14 cells/mm^2.

For mESC cultured in Agarose, 5,000 control or 125,000 Mitomycin treated cells were suspended in a 37 ℃ warmed 20 μL 0.5% low melting point Agarose (16520, Invitrogen) droplet at the bottom of the μ-slide 8 well dish. The dish was left at room temperature for 5 minutes to solidify and topped with the N2B27 medium. The cells were then culture at 37 ℃, 5% CO_2 till analysis.

For cells culture on E-cadherin-FC and fibronectin coated glass, the μ-slide 8 well dish was incubated with nitrocellulose/methanal at 37℃ for 3 hours and then was left air dried. The dish was then incubated with 10μg/mL E-cadherin-FC or fibronectin at 4℃ overnight. The dish was briefly washed with water. Mitomycin C pre-treated ES-E14 cells were seeded onto the dish at 14 cells/mm^2 in N2B27 medium. The cells were allowed to attach to the glass at 37 ℃ for one hour, then the medium was renewed to N2B27 medium with 20% Matrigel. The cells were fixed 24 hours post the Matrigel introduction.

For Mitomycin C treatment, the cells were incubated with 10 μg/mL Mitomycin C (J63193, Alfa Aesar) in culture media at 37 ℃ for two hours. The Mitomycin C contained media were removed and the cells were washed with PBS briefly. Then the Mitomycin C treated cells were trypsinized and subjected to further experiments.

Compositions of the culture media were as follows. Feeder Cell Medium: DMEM (41966, Thermo Fisher Scientific), 15% FBS (Stem Cell Institute), penicillin–streptomycin (15140122, Thermo Fisher Scientific), GlutaMAX (35050061, Thermo Fisher Scientific), MEM non-essential amino acids (11140035, Thermo Fisher Scientific), sodium pyruvate (11360070, Thermo Fisher Scientific) and 100 μM β-mercaptoethanol (31350-010,

Thermo Fisher Scientific). N2B27 Medium: 1:1 mix of DMEM F12 (21331-020, Thermo Fisher Scientific) and neurobasal A (10888-022, Thermo Fisher Scientific) supplemented with 2% v/v B27 (10889-038, Thermo Fisher Scientific), 0.2% v/v N2 (17502048, Gibco), 100 μM β-mercaptoethanol (31350-010, Thermo Fisher Scientific), penicillin–streptomycin (15140122, Thermo Fisher Scientific) and GlutaMAX (35050061, Thermo Fisher Scientific).

Immunofluorescence

Cells cultured in a μ-slide 8 well dish were fixed with 4% paraformaldehyde (J61899, Alfa Aesar) for 30 minutes at room temperature, then were permeabilised with 0.5% Triton X-100 for 15 minutes at room temperature. The cells were blocked with the incubation buffer (0.5% BSA, 0.1% Tween in PBS) for two hours, then were incubated with primary antibodies diluted in the incubation buffer at 4 ℃ overnight on shaking. The primary antibodies were washed off with PBS, then were incubated with secondary antibodies diluted in the incubation buffer at room temperature for two hours. The secondary antibodies were washed off with PBS. Samples cultured in the Matrigel were kept in PBS; samples cultured in Agarose were sealed in 200 μL 0.5% Agarose. The samples were imaged shortly after. Antibodies and dilutions were as listed below.

Primary antibody list

Protein	Catalog number	Type	Specie	Dilutions/Concentrations
E-cadherin	ECCD-2	Monoclonal	Rat	2 μg/mL
GM130	610822	Polyclonal	Mouse	1:300
OTX2	AF1979	Polyclonal	Goat	1:300
Podocalyxin	MAB1556	Monoclonal	Rat	3.3 μg/mL
PAR-3	07-330	Polyclonal	Rabbit	1:100
P-cadherin	AF761	Polyclonal	Goat	1:500
Γ-Tubulin	T6557	Monoclonal	Mouse	1:250
ZO-1	61-7300	Polyclonal	Rabbit	1:500

Secondary antibody list

Name	Target	Dilutions/Concentrations
Alexa Fluor 488	Rat	1:500
Alexa Fluor 488	Rabbit	1:500
Alexa Fluor 488	Goat	1:500
Alexa Fluor 546	Mouse	1:500
DyLight 550	Rat	1:500
CF 633	Phalloidin	6.6 pM

Microscope imaging

Live cell imaging was carried out on the PerkinElmer UltraVIEW spinning disk system fitted on an Olympus IX80 confocal microscope with a 37 ℃ and 5% CO_2 chamber. Images were captured with the 40x 1.3 NA (oil) objective, 2x Hamamatsu Orca-R2 CCD camera and Volocity 3.7.1 software. The cells were imaged at 2 μm z-step size and 30 minutes time intervals. Fixed samples were imaged on the Leica SP8 confocal microscope with the 40x 1.3 NA (oil) or 63x 1.4 NA (oil) objective and LAS X 3.7.4 software. The cells were imaged at 0.3 μm z-step size and 2X line average.

Image and data analysis

The central section images were projected from raw images in the Fiji software by maximum-value projection of the whole z stacks to produce the 3D projection images, or of the central three image of the z stacks to produce the central-section images. The whole z stacks projections were applied to count clump percentages. The central-section images were applied for line-scans to determine protein signals.

The mESCs with positive or negative protein centres were manually determined and counted. The percentage was calculated with the number relative to the number of total clumps captured in each condition. The mean percentages from three independent experiments were compared with student's t-test or one-way ANOVA specified in figure legends using the GraphPad Prism software. Sample sizes are specified in figure legends.

To quantify PAR-3 signal along the cell-cell interface, a 0.8μm width line was drawn alone the cell-cell interface by using F-ACTIN or E-CADHERIN signal as the path. PAR-3 and F-ACTIN Pixel values along the path were extracted. The two peaks of F-ACTIN signals at two ends of the path were determined as the start of end of the cell-cell interface and the positions in-between were defined as 1X cell-cell interface. The correspondent PAR-3 pixel to the F-ACTIN peak positions were identified and the PAR-3 line profile between the two positions were sectioned to 20 sections. PAR-3 pixel value in each section was averaged to be the PAR-3 signal in 5% of the cell-cell interface. The values from 10-15 cells were plotted as line graphs.

To compare the level of PAR3 in the core areas in the cells culture on the glass, a 6 μm diameter circular area of interest was created in the Fiji software to cover the PAR3 core area in a cell, and the average PAR3 fluorescence values in the circle was measured. The boundary of the cell was drawn by the free-hand tool in Fiji, and the average PAR3 fluorescence values in the boundary was measured. The ratio between the PAR3 values in the circle and inside the boundary was then calculated.

Supplementary Material and Methods

Line-scan analysis of E-cadherin

To quantify E-cadherin level along the cell membrane, the central z-stack from confocal microscope raw images was extracted. On that image, a line of 30-pixel wide were drawn perpendicular against the cell-cell membrane or cell-ECM membrane in Fiji. The peak fluorescence value of E-cadherin was extract from the line-scan profile. Three line-scans were done at different regions of the cell-cell membrane in one 2-cell clump, and three line-scans were done at the cell-ECM membrane in each cell of the 2-cell clump. The average value

of the three or six line-scans was regarded as the E-cadherin level at the cell-cell membrane or the cell-ECM membrane of that 2-cell clump.

Analysis of nuclear Otx2

To quantify nuclear Otx2 level, raw images were captured on the confocal microscope with Otx2 and DAPI channels. The raw images that contained z-axis stacks were subjected to maximum value projections in Fiji. The DAPI channel was turned into a binary image and the region under DAPI signals were masked by using the Analyse Particles tool in Fiji. The total Otx2 fluorescence values in each cell that were under the correspondent DAPI mask was measured and regarded as the Otx2 level of that cell.

Acknowledgements

We are grateful to Jon Clarke and Ben Steventon for critical reading of the manuscript and other members of the Buckley and Zernicka-Goetz labs for scientific discussion, especially Matteo Molè and Marta Shahbazi.

Funding: This research was financially supported by: CB - the Wellcome Trust and Royal Society (Sir Henry Dale Fellowship grant no. 208758/Z/17/Z and Dorothy Hodgkin Fellowship grant no. DH160086), XL - European Union's Horizon 2020 programme (Marie Skłodowska-Curie Individual Fellowship grant no. 844330), the Issac Newton Trust and Leverhulme Trust (Leverhulme Early Career Fellowship grant no. ECF-2019-175). AW and MZG: Wellcome Trust and ERC.

Thank you to the Cambridge Advanced Imaging Centre and the Paluch lab for help and access to confocal microscopy.

Author contributions: Conceptualisation: XL, CEB. Methodology: XL, AW. Formal analysis: XL, CYH. Investigation: XL, AW. Writing: XL, CEB. Visualisation: XL. Supervision: MZG, CEB. Funding acquisition: XL, AW, MZG, CEB.

References

Akhtar, N., and Streuli, C.H. (2013). An integrin--ILK--microtubule network orients cell polarity and lumen formation in glandular epithelium. Nat Cell Biol *15*, 17–27.

Bedzhov, I., and Zernicka-Goetz, M. (2014). Self-organizing properties of mouse pluripotent cells initiate morphogenesis upon implantation. Cell *156*, 1032–1044.

Blasky, A.J., Mangan, A., and Prekeris, R. (2015). Polarized protein transport and lumen formation during epithelial tissue morphogenesis. Annu Rev Cell Dev Biol *31*, 575–591.

Bryant, D.M., Datta, A., Rodriguez-Fraticelli, A.E., Peranen, J., Martin-Belmonte, F., and Mostov, K.E. (2010). A molecular network for de novo generation of the apical surface and lumen. Nat Cell Biol *12*, 1035–1045.

Bryant, D.M., Roignot, J., Datta, A., Overeem, A.W., Kim, M., Yu, W., Peng, X., Eastburn, D.J., Ewald, A.J., Werb, Z., et al. (2014). A molecular switch for the orientation of epithelial cell polarization. Dev Cell *31*, 171–187.

Buckley, C.E., Ren, X., Ward, L.C., Girdler, G.C., Araya, C., Green, M.J., Clark, B.S., Link, B.A., and Clarke, J.D.W. (2013). Mirror-symmetric microtubule assembly and cell interactions drive lumen formation in the zebrafish neural rod. Embo J *32*, 30–44.

Ciruna, B., Jenny, A., Lee, D., Mlodzik, M., and Schier, A.F. (2006). Planar cell polarity signalling couples cell division and morphogenesis during neurulation. Nature *439*, 220–224.

Herrera, A., Menendez, A., Torroba, B., Ochoa, A., and Pons, S. (2021). Dbnl and β-catenin promote pro-N-cadherin processing to maintain apico-basal polarity. J Cell Biol *220*, e202007055.

Iden, S., Rehder, D., August, B., Suzuki, A., Wolburg-Buchholz, K., Wolburg, H., Ohno, S., Behrens, J., Vestweber, D., and Ebnet, K. (2006). A distinct PAR complex associates physically with VE-cadherin in vertebrate endothelial cells. Embo Rep *7*, 1239–1246.

Ishida, S., Tanaka, R., Yamaguchi, N., Ogata, G., Mizutani, T., Kawabata, K., and Haga, H. (2014). Epithelial Sheet Folding Induces Lumen Formation by Madin-Darby Canine Kidney Cells in a Collagen Gel. Plos One *9*, e99655.

Jia, L., Liu, F., Hansen, S.H., Beest, M.B.A. ter, and Zegers, M.M.P. (2011). Distinct roles of cadherin-6 and E-cadherin in tubulogenesis and lumen formation. Mol Biol Cell *22*, 2031–2041.

Kim, Y.S., Fan, R., Kremer, L., Kuempel-Rink, N., Mildner, K., Zeuschner, D., Hekking, L., Stehling, M., and Bedzhov, I. (2021). Deciphering epiblast lumenogenesis reveals proamniotic cavity control of embryo growth and patterning. Sci Adv *7*, eabe1640.

Klinkert, K., Rocancourt, M., Houdusse, A., and Echard, A. (2016). Rab35 GTPase couples cell division with initiation of epithelial apico-basal polarity and lumen opening. Nat Commun *7*, 11166.

Larue, L., Antos, C., Butz, S., Huber, O., Delmas, V., Dominis, M., and Kemler, R. (1996). A role for cadherins in tissue formation. Development *122*, 3185–3194.

Li, D., Mangan, A., Cicchini, L., Margolis, B., and Prekeris, R. (2014). FIP5 phosphorylation during mitosis regulates apical trafficking and lumenogenesis. Embo Rep *15*, 428–437.

Luján, P., Varsano, G., Rubio, T., Hennrich, M.L., Sachsenheimer, T., Gálvez-Santisteban, M., Martín-Belmonte, F., Gavin, A.-C., Brügger, B., and Köhn, M. (2016). PRL-3 disrupts epithelial architecture by altering the post-mitotic midbody position. J Cell Sci *129*, 4130–4142.

Mangan, A.J., Sietsema, D.V., Li, D., Moore, J.K., Citi, S., and Prekeris, R. (2016). Cingulin and actin mediate midbody-dependent apical lumen formation during polarization of epithelial cells. Nat Commun *7*, 12426.

Molè, M.A., Weberling, A., Fässler, R., Campbell, A., Fishel, S., and Zernicka-Goetz, M. (2021). Integrin β1 coordinates survival and morphogenesis of the embryonic lineage upon implantation and pluripotency transition. Cell Reports *34*, 108834.

Morais-de-Sa, E., Mirouse, V., and Johnston, D.S. (2010). aPKC phosphorylation of Bazooka defines the apical/lateral border in Drosophila epithelial cells. Cell *141*, 509–523.

Nikolopoulou, E., Galea, G.L., Rolo, A., Greene, N.D.E., and Copp, A.J. (2017). Neural tube closure: cellular, molecular and biomechanical mechanisms. Development *144*, 552–566.

Noordstra, I., Hermoso, M.D., Schimmel, L., Bonfim-Melo, A., Kalappurakkal, J.M., Mayor, S., Gordon, E., Cusachs, P.R., and Yap, A.S. (2021). Cortical actin flow activates an α-catenin clutch to assemble adherens junctions. Biorxiv 2021.07.28.454239.

Quesada-Hernandez, E., Caneparo, L., Schneider, S., Winkler, S., Liebling, M., Fraser, S.E., and Heisenberg, C.P. (2010). Stereotypical Cell Division Orientation Controls Neural Rod Midline Formation in Zebrafish. Curr Biol *20*, 1966–1972.

Rathbun, L.I., Colicino, E.G., Manikas, J., O'Connell, J., Krishnan, N., Reilly, N.S., Coyne, S., Erdemci-Tandogan, G., Garrastegui, A., Freshour, J., et al. (2020). Cytokinetic bridge triggers de novo lumen formation in vivo. Nat Commun *11*, 1269.

Schlüter, M.A., Pfarr, C.S., Pieczynski, J., Whiteman, E.L., Hurd, T.W., Fan, S., Liu, C.-J., and Margolis, B. (2009). Trafficking of Crumbs3 during cytokinesis is crucial for lumen formation. Mol Biol Cell *20*, 4652–4663.

Shahbazi, M.N., Scialdone, A., Skorupska, N., Weberling, A., Recher, G., Zhu, M., Jedrusik, A., Devito, L.G., Noli, L., Macaulay, I.C., et al. (2017). Pluripotent state transitions coordinate morphogenesis in mouse and human embryos. Nature *552*, 239–243.

Soncin, F., Mohamet, L., Eckardt, D., Ritson, S., Eastham, A.M., Bobola, N., Russell, A., Davies, S., Kemler, R., Merry, C.L.R., et al. (2009). Abrogation of E-Cadherin-Mediated Cell–Cell Contact in Mouse Embryonic Stem Cells Results in Reversible LIF-Independent Self-Renewal. Stem Cells *27*, 2069–2080.

Symonds, A.C., Buckley, C.E., Williams, C.A., and Clarke, J.D.W. (2020). Coordinated assembly and release of adhesions builds apical junctional belts during de novo polarisation of an epithelial tube. Development *147*, dev191494.

Tawk, M., Araya, C., Lyons, D.A., Reugels, A.M., Girdler, G.C., Bayley, P.R., Hyde, D.R., Tada, M., and Clarke, J.D. (2007). A mirror-symmetric cell division that orchestrates neuroepithelial morphogenesis. Nature *446*, 797–800.

Wang, L.-T., Rajah, A., Brown, C.M., and McCaffrey, L. (2021). CD13 orients the apical-basal polarity axis necessary for lumen formation. Nat Commun *12*, 4697.

Wang, T., Yanger, K., Stanger, B.Z., Cassio, D., and Bi, E. (2014). Cytokinesis defines a spatial landmark for hepatocyte polarization and apical lumen formation. J Cell Sci *127*, 2483–2492.

Yu, W., Datta, A., Leroy, P., O'Brien, L.E., Mak, G., Jou, T.S., Matlin, K.S., Mostov, K.E., and Zegers, M.M. (2005). Beta1-integrin orients epithelial polarity via Rac1 and laminin. Mol Biol Cell *16*, 433–445.

Zhang, Y., Mets, R.D., Monzel, C., Acharya, V., Toh, P., Chin, J.F.L., Hul, N.V., Ng, I.C., Yu, H., Ng, S.S., et al. (2020). Biomimetic niches reveal the minimal cues to trigger apical lumen formation in single hepatocytes. Nat Mater *19*, 1026–1035.

Zigman, M., le, A.T., Fraser, S.E., and Moens, C.B. (2011). Zebrafish neural tube morphogenesis requires scribble-dependent oriented cell divisions. Curr Biol *21*, 79–86.

Figures

Figure 1

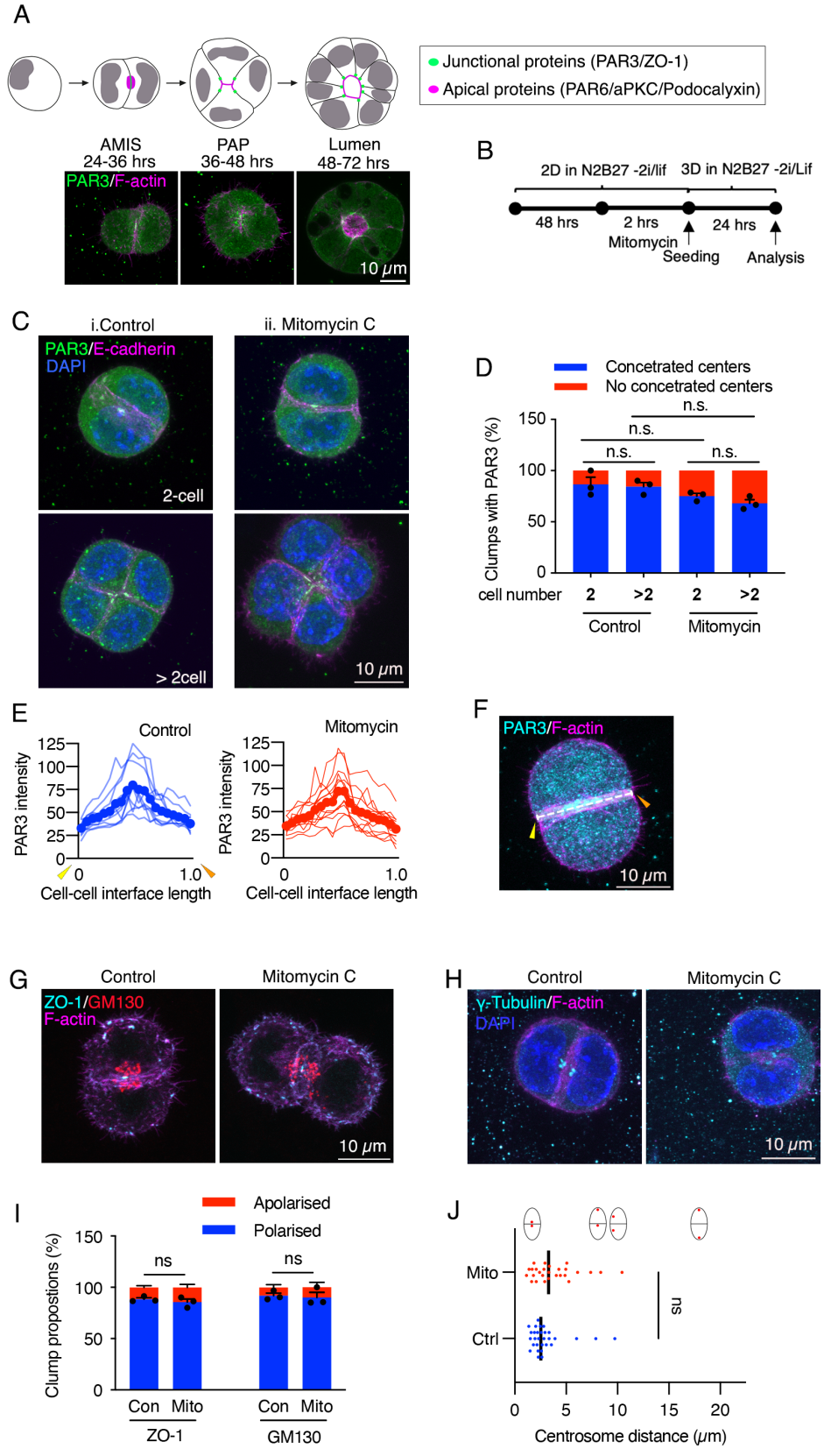

Figure 1. Cell division is dispensable for mouse embryonic stem cells (mESC) in Matrigel 3D cultures.

(A) Stages of polarisation and lumen formation in mESCs cultured in Matrigel
(B) Timeline of experiment setups to assess AMIS formation.
(C) Immunofluorescence of PAR3. A polarised, concentrated PAR3 center was formed in 2-cell mESC clumps and 3- or 4-cell mESC in both control and Mitomycin treated conditions.
(D) Quantification of the frequency of cell clumps with a polarised Pard3 centre. N=3 experiments, at least 25 clumps were analysed for each column in every experiment. Data are means ± SEM, one-way ANOVA analysis; n.s., not significant.
(E) Line-scans of Pard3 at the cell-cell interface of 2-cell mESC clumps. Line scans were sections and fitted to each 5% along the cell-cell interface length. 12 lines scans from one experiment were and profiled for each condition.
(F) An example and illustration of the line-scan analysis in E. The line-scan profiles were from the yellow arrow to the orange arrow.
(G) Representative images of concentrated ZO-1 dot and polarised Golgi apparatus (labelled by GM130).
(H) Immunofluorescence of γ-tubulin in mESCs to label centrosomes.
(I) Quantification of the frequency of cell clumps with a polarised ZO-1 or Golgi apparatus centre. N=3 experiments, at least 25 clumps were analysed for each column in every experiment. Data are means ± SEM, student's t-test analysis; n.s., not significant.
(J) Distance between centrosomes in paired mESCs in 2-cell mESC clumps. N = 35 clumps in each condition. Data with the median values, student's t-test analysis; n.s., not significant.

Figure 2

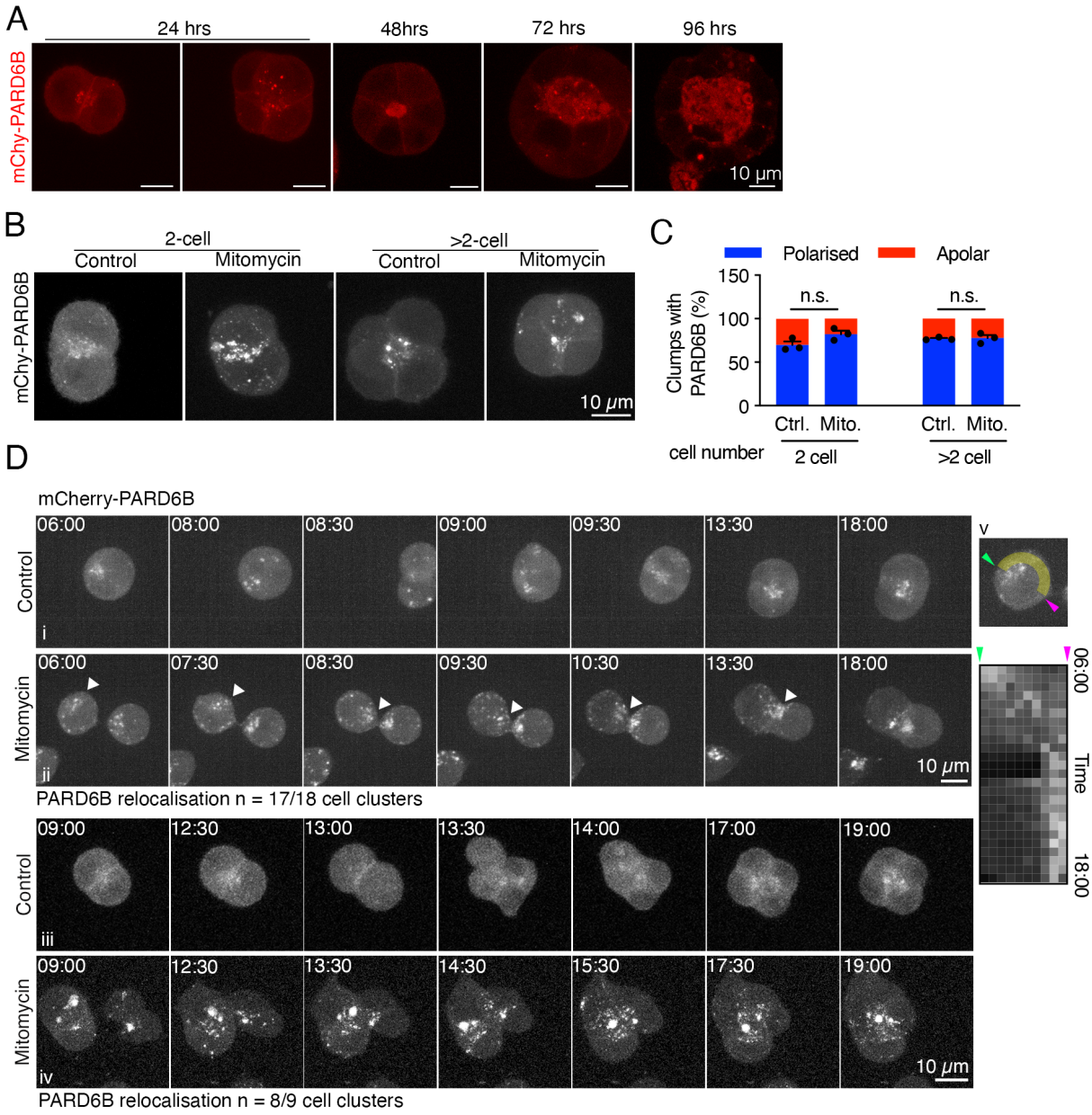

Figure 2. Polarised Pard6B in mESC 3D cultures

(A) Live cell imaging of mCherry-PAR6B mESC control cells cultured from 24 – 96 hours in Matrigel.

(B) Representative live cell images of mCherry-PAR6B in mESCs upon 24 hours in Matrigel.

(C) Quantification of the frequency of cell clumps with polarised mCherry-Pard6B. N=3 experiments, at least 25 clumps were analysed for each column in every experiment. Data are means ± SEM, student's t-test analysis; n.s., not significant.

(D) Movie stills of mCherry-PAR6B in control and Mitomycin C treated mESCs cultured in Matrigel (also Supplementary Movie 2). Control cells divided (i) and two mitomycin treated cells touched (ii) to form 2-cell clumps. Control cells divided twice (iii) and two mitomycin treated cell clumps touched (iv) to form 4-cell clumps. (v), Kymograph of mCherry-PAR6B in the arrow-head cell in (ii) along the path between the arrows; each pixel is the fluoresce values averaged in 0.2 μm sections.

Figure 3

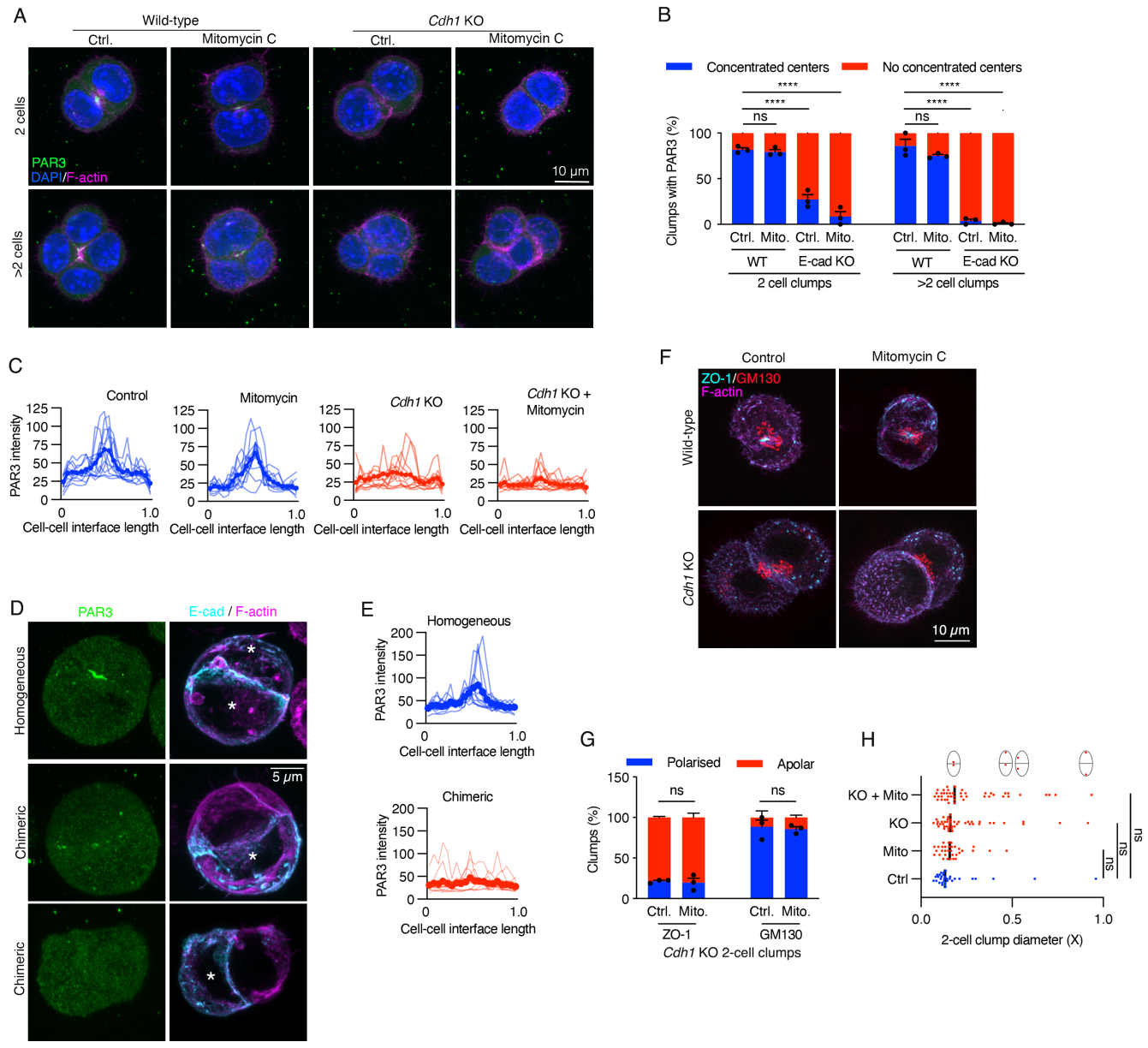

Figure 3. E-cadherin junctions are important for polarisation.

(A) Immunofluorescence of PAR3 in wild-type and E-cadherin knock-out (Cdh1 KO) cells at 24 hrs in Matrigel.

(B) Proportions of mESC clumps with a positive Pard3 centre. N=3 experiments, at least 25 clumps were analysed for each column in every experiment. Data are means ± SEM, one-way ANOVA; n.s., not significant, ****, P<0.0001.

(C) Line-scan profiles of PAR3 at the cell-cell interface in wild-type control, mitomycin C treated and Cdh1 KO control, mitomycin C treated 2-cell clumps. N = 12 clumps in each condition.

(D) Representative images of ZO-1 dot and Golgi apparatus (labelled by GM130) in WT and Cdh1 KO mESC clumps.

(E) Proportions of mESC clumps with a central ZO1 dot or polarised Golgi apparatus. N=3 experiments, at least 25 clumps were analysed for each column in every experiment. Data are means ± SEM, students' t test; n.s., not significant.

(F) Distance between centrosomes in paired mESCs in 2-cell mESC clumps. N = 35-40 clumps in each condition. Data with the median values, student's t-test analysis; n.s., not significant.

(G) Representative images of PAR3 immunofluorescence in WT homogeneous or WT/Cdh1 KO chimeric mESC 2-cell clumps.

(H) Line-scan profiles of PAR3 at the cell-cell interface of homogeneous and chimeric mESC 2-cell clumps. N = 11 clumps in each condition.

Figure 4

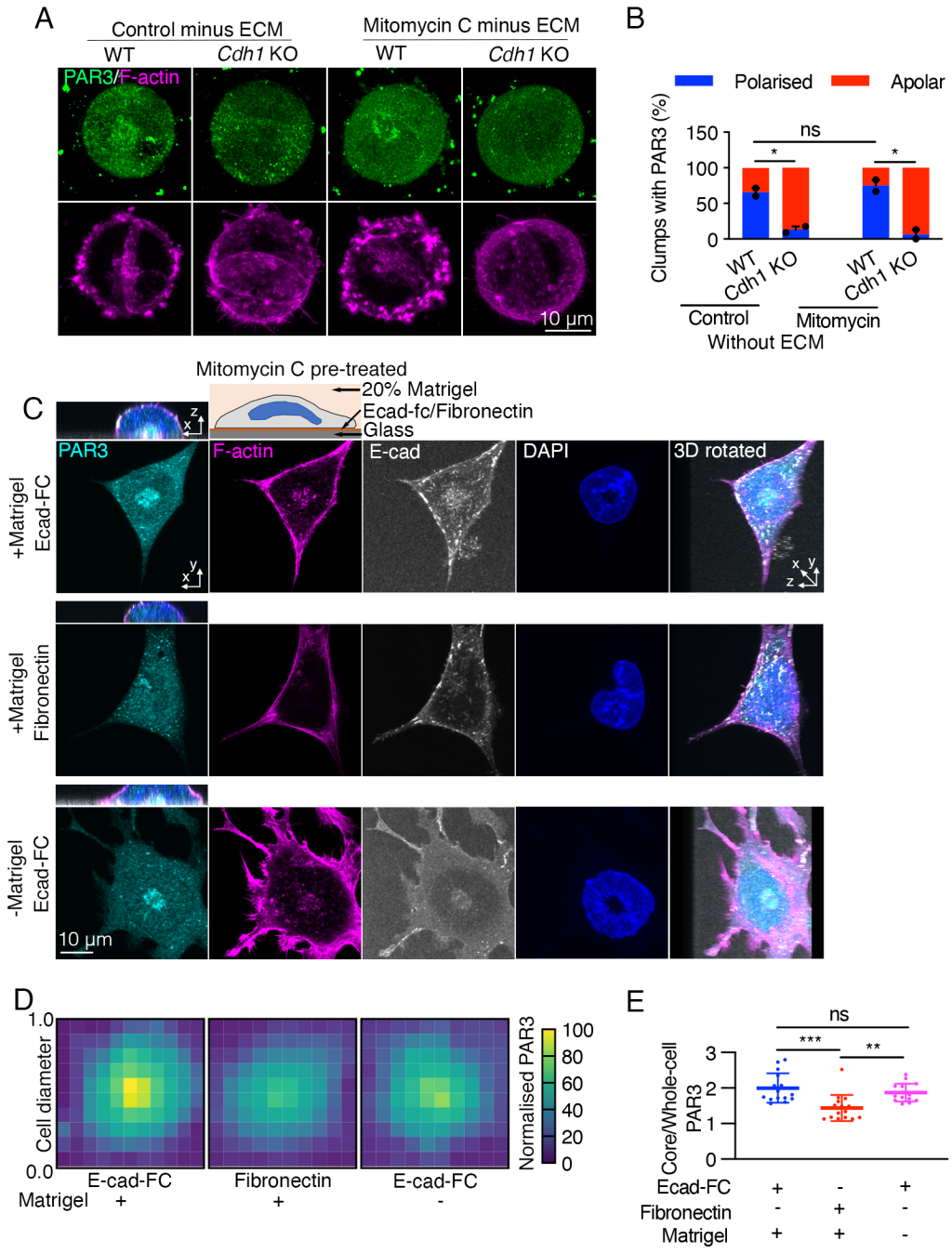

Figure 4. Cell-ECM interactions in regulating AMIS seeding.

(A) Immunofluorescence of PAR3 in wild-type and E-cadherin knock-out (Cdh1 KO) cells at 30 hours in Matrigel.

(B) Proportions of mESC clumps with polarised PAR3. N=2 experiments, at least 15 clumps were analysed for each column in every experiment. Data are means ± SEM, one-way ANOVA; n.s., not significant, *, P<0.05.

(C) Immunofluorescence of PAR-3 in cell division blocked mESCs cultured against E-cadherin-FC or Fibronectin coated glass topped with or without Matrigel for 24 hours.

(D) Heatmap of PAR3 in cell from the experiment of (C). Squared frames were fitted to the main bodies of the cells and average values in each 10% along the width of the frames was calculated as a pixel. The heatmaps were stacks of 15 cells in one experiment. The values were normalised to the peak value in the E-cad-FC plus Matrigel condition.

(E) Ratios between PAR3 in the 2.5 μm diameter central core and whole cell surface. N = 15 cells in one experiment. Data are means ± SEM, one-way ANOVA; n.s., not significant, **, P<0.01, ***, P<0.001.

Figure 5

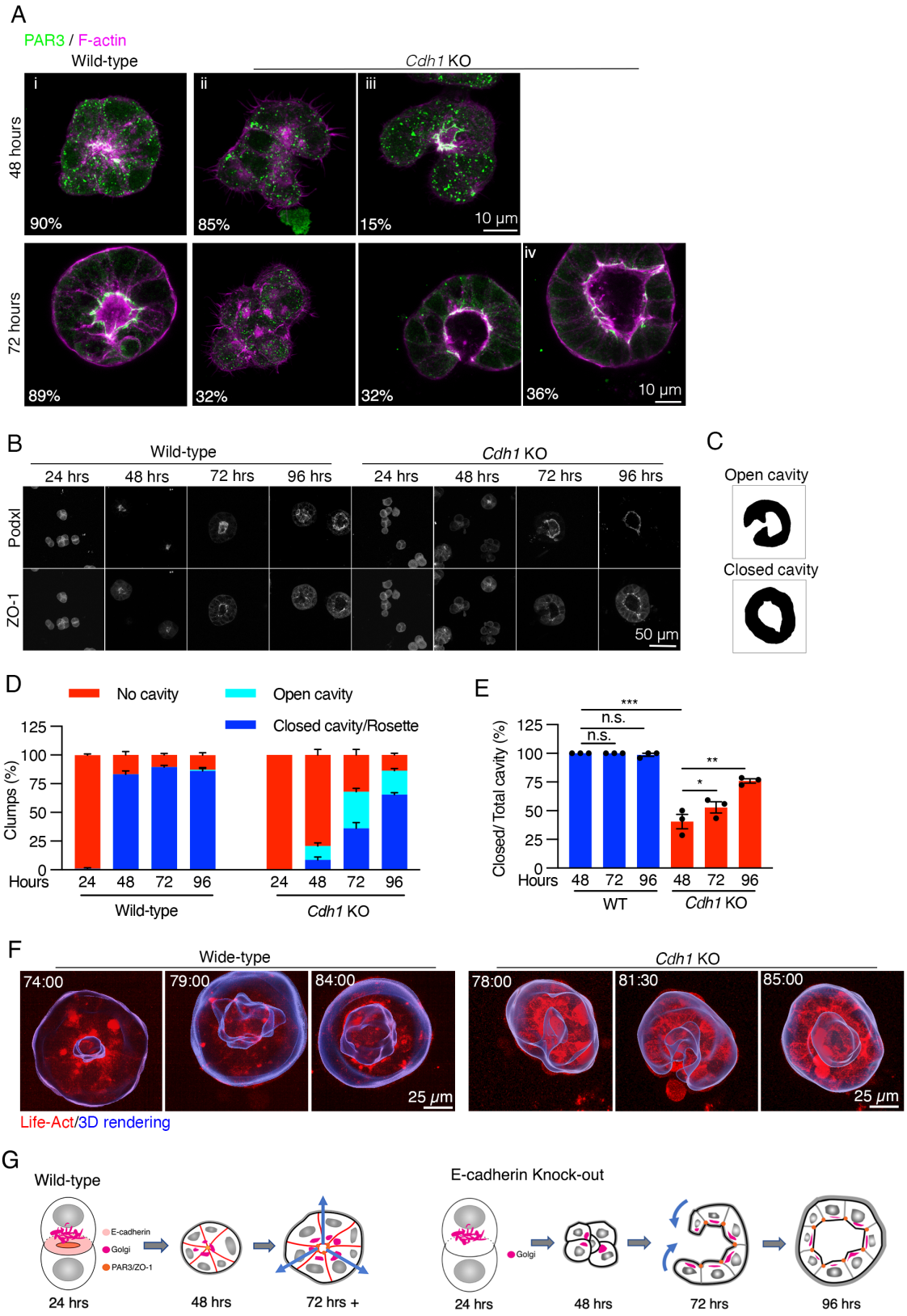

Figure 5. Lumenogenesis in wild-type and E-cadherin knock-out mESC cultures.

(A) PAR3 immunofluorescence in wild-type mESC that form polarised rosettes or lumen (i); and Cdh1 KO mESC that did not form AMIS (ii), polarised PAR3 (iii), or lumeninal PAR3 (iv) when cultured in Matrigel for 48 and 73 hours. The percentages were quantified from one experiment,

(B) Podocalyxin (Podxl) and ZO-1 stainings in WT and Cdh1KO mESCs cultured in Matrigel from 1-4 days.
(C) Exampled masking cell occupied areas of different types of spheroids extracted from the Cdh1 KO mESCs at 72 and 96 hrs. The spheroids were catalogued into two types with open and closed cavities based on Podocalyxin signals.
(D) Percentage of clumps with different cavities relative to total cell clusters in different time points. N=3 experiments, at least 25 clumps were analysed for each column in every experiment. Data are means ± SEM, one-way ANOVA analysis.
(E) Percentage of clumps with close cavities relative to total spheroids with cavities calculated from (D).
(F) Movies stills of LifeAct-mRuby labelled cell clusters. Images are overlaid with 3D rendering of the cluster surfaces. The images are 50 μm-depth projection alongs the z-axis of imaging.
(G) Illustration of lumenogenesis in WT and Cdh1 KO mESCs.

Supplementary Figures

Figure S1

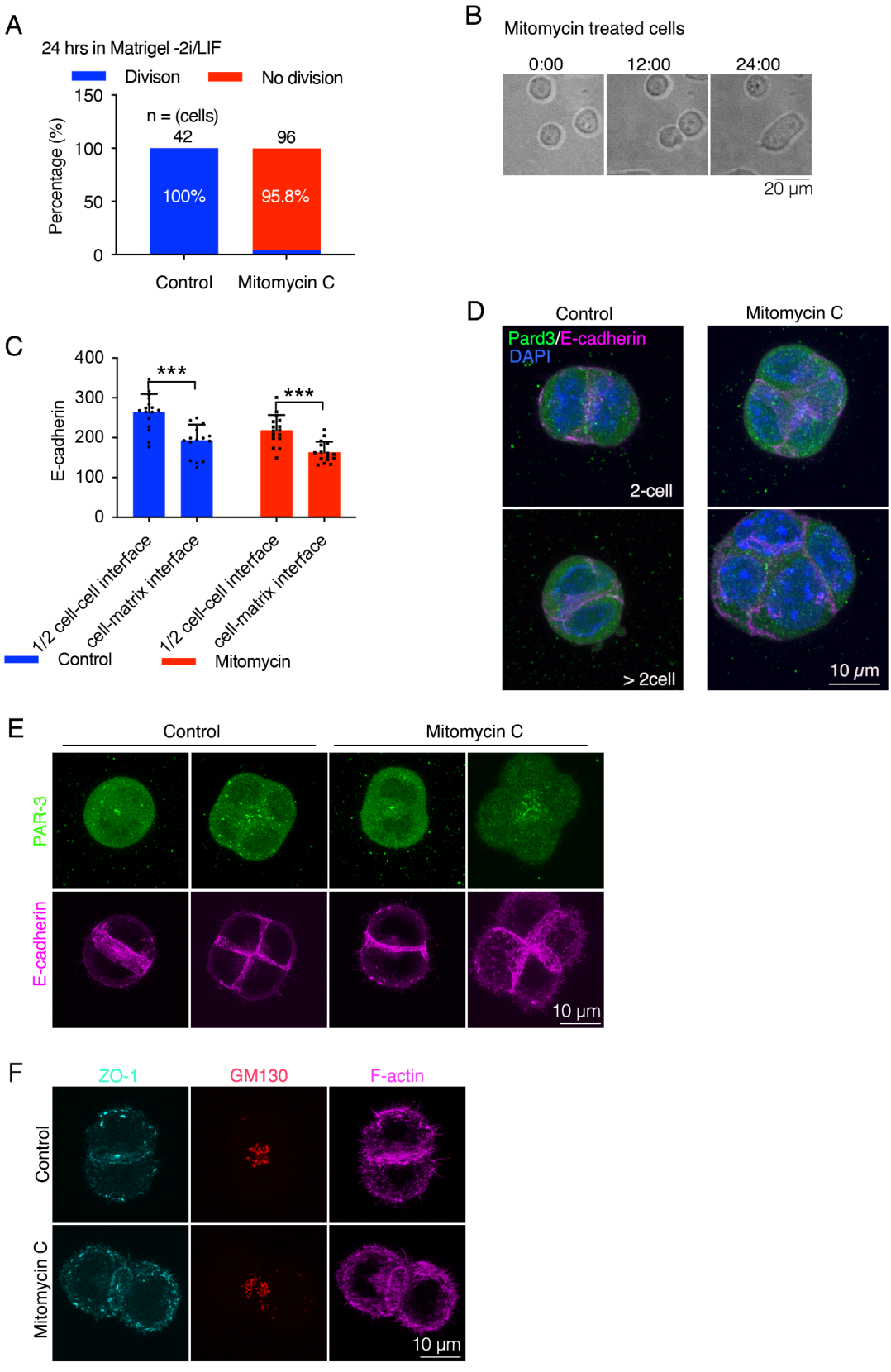

Figure S1. Division blocked mouse embryonic stem cells (mESC) formed E-cadherin cell-cell contacts in Matrigel 3d cultures.

(A) Mitomycin C sufficiently blocked cells divisions. Track of cells experienced cell divisions or did not experience cell divisions for live movies in the first 24 hours upon seeding into Matrigel by live cell imaging. N equals to total numbers of cells tracked at time point zero.

(B) Movie stills of Mitomycin treated cells from Supplemental Movie 1.

(C) Quantification of E-cadherin fluorescence intensity at cell-cell interfaces and cell-matrix interfaces. N = 18 clumps in each condition. Data are means ± SEM, student's t-test; ***, P<0.001.

(D) Representative images of mESCs that were negative of PAR3 centres.

(E) Split-channel images of Figure 1C.

(F) Split-channel images of Figure 1G, H.

Figure S2

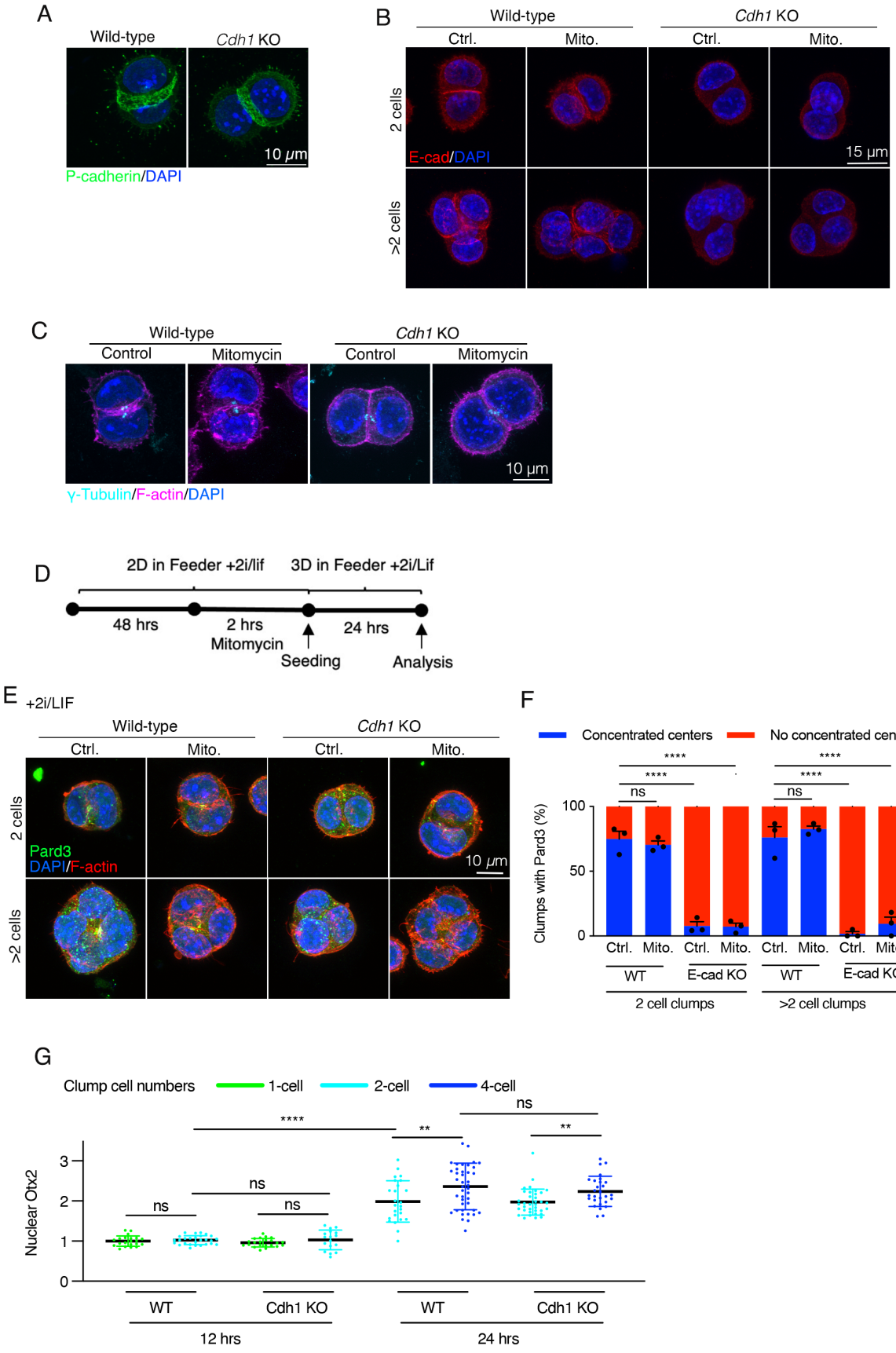

Figure S2. ZO-1 and Golgi network (GM130) in wild-type and E-cadherin knock-out clumps.

(A) Immunofluorescence of P-cadherin in wild-type and E-cadherin KO mESCs cultured 24 hours in Matrigel.
(B) Both wild-type and E-cadherin KO mESCs form cell clusters when untreated or after Mitomycin treatment.
(C) Representative images of centrosomes in wild-type and E-cadherin KO mESCs cultured 24 hours in Matrigel with or without cell divisions.
(D) Timeline of experiment setups to assess *de novo* polarisation when the mESC cultured with 2i/Lif to remain pluripotent.
(E) Immunofluorescence of Pard3 in wild-type and E-cadherin KO mESCs cultured in Matrigel for 24 hours with 2i/Lif.
(F) Quantification of the frequency of cell clumps with a polarised Pard3 centre. N=3 experiments, at least 25 clumps were analysed for each column in every experiment. Data are means ± SEM, one-way ANOVA analysis; ns, not significant, ****, P<0.0001.
(G) Nuclear levels of Otx2 based on immunofluorescence in wild-type and E-cadherin KO mESCs after or without cell divisions at 12 or 24 hours post seeding into Matrigel. Only cells that were not undergoing cell divisions were analysed. N = 22-42 cells in each column from one experiment. Data are means ± SEM, one-way ANOVA analysis. ns, not significant, **, P<0.01, ****, P<0.0001.

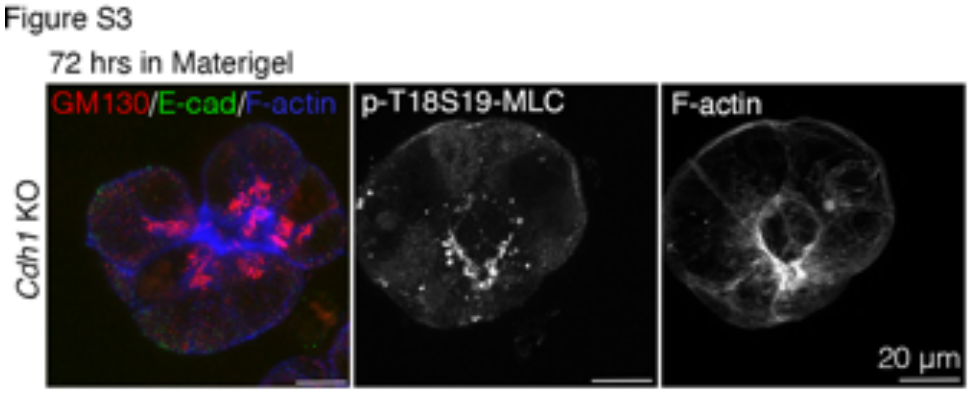

Figure S3. The Golgi network, phor-myosin light chain 2 and F-actin in E-cadherin knock-out cells cultured 72 hours in Matrigel.

Supplementary Movies

Supplementary Movie 1. Dividing and division-blocked mESCs cultured in Matrigel.

Bright-field live movies of left, control and right Mitomycin C treated mESCs cultures in Matrigel from 0 – 24 hours. The control cells divided once or two times while the treated cells had no divisions.

Supplementary Movie 2. Representative movies of mCherry-Pard6B in dividing and division-blocked mESCs cultured in Matrigel

Top, mESCs cultured in Matrigel formed 2-cell clumps from 6 – 18 hours in Matrigel; Bottom, Top, mESCs cultured in Matrigel formed 2-cell clumps from 9 – 19 hours in Matrigel.

Supplementary Movie 3. Representative movies of cysts forming in wild-type and E-cadherin knock-out mESCs cultured in Matrigel

Left, wild-type mESCs cultured from 74 – 84 hours, interval = 1 hour; Right and E-cadherin knock-out mESCs cultured from 78 – 85 hours, interval = 30 min. The cells expressed LifeAct-mRuby.

Supplementary Movie 4. Rotation of the 3D rendering in Figure 5F.

Left, Cdh1KO mESCs cultured 78 hours; Middle, 81.5 hours; Right, 85 hours in Matrigel.